

**Quantitative CH<sub>2</sub>I<sub>2</sub>  
vapor spectrum**

T. J. Johnson et al.

# The quantitative infrared and NIR spectrum of CH<sub>2</sub>I<sub>2</sub> vapor: vibrational assignments and potential for atmospheric monitoring

**T. J. Johnson, T. Masiello, and S. W. Sharpe**

Pacific Northwest National Laboratory, Richland, WA 99354, USA

Received: 15 November 2005 – Accepted: 3 January 2006 – Published: 17 February 2006

Correspondence to: T. J. Johnson (timothy.johnson@pnl.gov)

© 2006 Author(s). This work is licensed under a Creative Commons License.

Title Page

Abstract

Introduction

Conclusions

References

Tables

Figures

◀

▶

◀

▶

Back

Close

Full Screen / Esc

Print Version

Interactive Discussion

EGU

## Abstract

Diiodomethane ( $\text{CH}_2\text{I}_2$ ) photolysis in the presence of ozone is a suggested precursor to new particle aerosol formation, particularly in coastal areas. As part of the PNNL database of gas-phase infrared spectra, the quantitative absorption spectrum of  $\text{CH}_2\text{I}_2$  has been acquired at  $0.1\text{ cm}^{-1}$  resolution. Two strong  $b_2$  symmetry A-type bands at  $584$  and  $1114\text{ cm}^{-1}$  are observed, but are not resolved at  $760\text{ Torr}$  and appear as B-type. In contrast, the  $b_1$  symmetry C-type bands near  $5953$ ,  $4426$  and  $3073\text{ cm}^{-1}$  are resolved with rotational structure, including Q-branches with widths  $\leq 1\text{ cm}^{-1}$ . The quantitative infrared and near-infrared vapor-phase spectra ( $600\text{--}10\,000\text{ cm}^{-1}$ ) are reported for the first time and discussed in terms of atmospheric monitoring. FT-Raman spectra and ab initio calculations are used to complete vibrational assignments in the  $\text{C}_{2v}$  point group.

## 1. Introduction

Twenty-five years ago Chameides and Davis (1980) suggested the potential importance of iodine in tropospheric chemistry. They recognized that certain species such as methyl iodide,  $\text{CH}_3\text{I}$ , are easily photolyzed to liberate atomic iodine, which can react with  $\text{O}_3$  and then  $\text{NO}_x$  or  $\text{HO}_x$  to form other inorganic species such as  $\text{IO}$ ,  $\text{HOI}$  or  $\text{IONO}_2$ :



Similar to the  $\text{ClO}_x$  and  $\text{BrO}_x$  systems, the various iodine species can be cycled back to a radical I atom with catalytic  $\text{O}_3$  destruction and an increase in the  $\text{NO}_2/\text{NO}$  ratio. Subsequent works continue to emphasize the importance of iodine in atmospheric

## Quantitative $\text{CH}_2\text{I}_2$ vapor spectrum

T. J. Johnson et al.

Title Page

Abstract

Introduction

Conclusions

References

Tables

Figures

◀

▶

◀

▶

Back

Close

Full Screen / Esc

Print Version

Interactive Discussion

chemistry (Solomon et al., 1994). Although typical concentrations are low (sub-ppb<sub>v</sub>), most organic iodides are readily photolyzed in the visible and near-UV and the ensuing kinetics are typically fast, thus leading to the importance of the iodine cycles.

In addition to CH<sub>3</sub>I, the photolysis of CH<sub>2</sub>I<sub>2</sub> was also investigated some years ago where it was suggested that I<sub>2</sub> appears as an end photoproduct and that (at high concentrations) there is significant regeneration of the parent compound (Schmitt and Comes, 1980; Kasper et al., 1964, 1965). More recently, the photolysis of CH<sub>2</sub>I<sub>2</sub> has had renewed interest since laboratory experiments have shown that the photolysis of certain iodine-containing species in the presence of ozone (O<sub>3</sub>) plays a role in the formation of aerosols (Jimenez et al., 2003; Kolb, 2002; Burkholder et al., 2004). This is important since field experiments have shown that the seas are a direct source of several gas-phase halogenated species, (McFiggans et al., 2004; Carpenter et al., 1999) including CH<sub>2</sub>I<sub>2</sub>. Diiodomethane and other alkyl iodides have been identified with maritime biogenic sources, (Carpenter et al., 1999) in particular *Laminaria* Macroalgae (McFiggans et al., 2004) or the brown algae *Fucus* (Mäkelä et al., 2002). Laboratory experiments (Cox et al., 1999; Hoffmann et al., 2001) have clearly indicated that iodine dioxide, OIO, is formed from the photochemistry of the radical intermediate IO, reacting either with itself (Harwood et al., 1997) or with the BrO radical (Gilles et al., 1997):



O'Dowd and co-workers have also shown that nucleation was observed over several orders of magnitude in CH<sub>2</sub>I<sub>2</sub> and suggested that the gas-phase OIO is responsible for the aerosol growth (Jimenez et al., 2003). New particle growth in coastal areas has shown the particles to be rich in iodine (Jimenez et al., 2003; Mäkelä et al., 2002) and this plays a role in marine boundary layer ozone loss (Vogt et al., 1999).

In terms of spectroscopy, relatively little has been reported regarding gas-phase CH<sub>2</sub>I<sub>2</sub>. The early photolysis work of Pimentel and co-workers (Kasper et al., 1964, 1965) as well as Kroger et al. (1976) and Schmitt and Comes (1980) showed that photolysis liberates an I atom and an internally excited CH<sub>2</sub>I radical. Vibrational spectra

## Quantitative CH<sub>2</sub>I<sub>2</sub> vapor spectrum

T. J. Johnson et al.

[Title Page](#)[Abstract](#)[Introduction](#)[Conclusions](#)[References](#)[Tables](#)[Figures](#)[◀](#)[▶](#)[◀](#)[▶](#)[Back](#)[Close](#)[Full Screen / Esc](#)[Print Version](#)[Interactive Discussion](#)

of CH<sub>2</sub>I<sub>2</sub> liquid have been reported previously by both Ford (1975) and Voelz and co-workers (1953), with all fundamentals being assigned in the C<sub>2v</sub> point group, as well as some combination and overtone bands. Although both the liquid- and vapor-phase spectra have been recorded in the IR, (Ford, 1975; Voelz et al., 1953), it appears the resolution was not sufficient to resolve any ro-vibronic structure in the vapor. There have also been assignments made of the  $\Delta\nu_{\text{CH}}=3, 4, 5$  and 6 overtones in the near-infrared spectrum, (Henry and Hung, 1978) but these were also in the liquid phase. For diiodomethane, the anharmonicity was used to extrapolate a fundamental frequency of 3059 cm<sup>-1</sup> for the liquid, which would correspond to the C-H stretch  $\nu_6$  fundamental (*vide infra*). To date there have been no quantitative spectra of the vapor of this moderately volatile species (1.2 Torr at 298 K).

The Pacific Northwest National Laboratory (PNNL) continues to construct a reference library of quantitative high-resolution infrared spectra designed for tropospheric monitoring (Sharpe et al., 2004). This Northwest Infrared (NWIR) database, is optimized for best signal-to-noise ratio (SNR) in the long-wave infrared (LWIR), 800–1300 cm<sup>-1</sup>, but each spectrum has a minimal spectral range of  $\leq 600$  to  $\geq 6500$  cm<sup>-1</sup>. When certain bands are recognized as having sufficient SNR outside this minimal spectral range, these data are also included. The reference spectra are intended primarily for open path monitoring; each laboratory measurement has the analyte back-pressurized with ultra-high purity (UHP) nitrogen to 760 $\pm$ 5 Torr. The data are nevertheless recorded at 0.112 cm<sup>-1</sup> resolution in the desire to bring out all possible spectral features, not only the resolved ro-vibronic lines of lighter species, but also the Q-branches of many polyatomics that display halfwidths of 1 cm<sup>-1</sup> or less. Recognizing that most species have typical pressure broadening coefficients of  $\sim 0.1$  cm<sup>-1</sup>/atm, additional resolution was deemed unnecessary for these reference data.

While constructing the NWIR database, it was recognized that CH<sub>2</sub>I<sub>2</sub> has recently garnered great interest among the atmospheric community, and it would be beneficial to point out a method for monitoring this trace gas. Since estimated maritime boundary layer concentrations are at most 100s of ppt<sub>v</sub>, it was recognized that the only optical

**Quantitative CH<sub>2</sub>I<sub>2</sub>  
vapor spectrum**

T. J. Johnson et al.

Title Page

Abstract

Introduction

Conclusions

References

Tables

Figures

◀

▶

◀

▶

Back

Close

Full Screen / Esc

Print Version

Interactive Discussion

methods with sufficient sensitivity to see CH<sub>2</sub>I<sub>2</sub> would be, for example, long path DOAS or narrow-band IR laser techniques (Johnson et al., 1991a; Sharpe et al., 1998). Special attention was thus paid to narrow spectral features: e.g., transitions over which a probing laser frequency can easily be tuned.

## 2. Experimental

Using the methods of Chu et al. (1999) and Sharpe et al. (2004) a series of measurements is made, each corresponding to a different concentration-path length burden. Each fitted spectrum, in fact, represents a series of (typically >10) individual measurements at 298.1 K, with the different measurements covering a large range (often >2 orders of magnitude) of analyte burdens, each burden pressurized with UHP N<sub>2</sub> to one atmosphere. The fitted spectrum is derived by fitting a Beer's law plot at each wavelength channel to each of the individual burdens (Chu et al., 1999). In order to account for any of several different nonlinearity phenomena, the individual burdens are weighted according to T<sup>2</sup> (where T=I/I<sub>0</sub>). All values with T < 0.025 (i.e. decadic absorbance > 1.6) are weighted with zero. This multiple burden with weighted data approach retains several advantages over any single measurement or few measurements: First, multiple measurements greatly enhance the SNR ratio. Second, the high burden measurements enhance the SNR for the weak bands that might not exceed the noise floor in any measurement designed to keep the strong bands on scale. Third, for the strong bands, the weighting mechanism brings out a better fidelity to account for Beer's law saturation effects, photoconductive detector nonlinearity effects or other phenomena that cause the absorbance values to not scale with burden. Finally, analyzing the residual vector has proven helpful at recognizing chemical impurities as their signatures typically do not scale with the fit.

The CH<sub>2</sub>I<sub>2</sub> sample was from Aldrich Chemicals and its purity was monitored by comparing to known infrared spectra. A Bruker IFS 66v/S vacuum spectrometer (Johnson et al., 2005) was used over the 600 to 6500 cm<sup>-1</sup> range. The spectrometer hardware

## Quantitative CH<sub>2</sub>I<sub>2</sub> vapor spectrum

T. J. Johnson et al.

Title Page

Abstract

Introduction

Conclusions

References

Tables

Figures

◀

▶

◀

▶

Back

Close

Full Screen / Esc

Print Version

Interactive Discussion

**Quantitative CH<sub>2</sub>I<sub>2</sub>  
vapor spectrum**

T. J. Johnson et al.

Title Page

Abstract

Introduction

Conclusions

References

Tables

Figures

◀

▶

◀

▶

Back

Close

Full Screen / Esc

Print Version

Interactive Discussion

EGU

characteristics have been previously documented (Johnson et al., 2002) according to IUPAC guidelines, (Bertie, 1998) taking care to avoid ghosting, “warm aperture” (Johnson et al., 2002) and detector nonlinearity (Chase, 1984; Birk et al., 1996) artifacts. Due to the modest vapor pressure of CH<sub>2</sub>I<sub>2</sub>, these measurements were made on a long path flowed system whereby the liquid analyte is quantitatively delivered into a heated stream of ultra-high purity N<sub>2</sub> carrier gas, (Sharpe et al., 2003; Johnson et al., 2006<sup>1</sup>) using a specially constructed vapor dissemination system. The measurement at 298.1 K is made in a specially designed White cell with a circulating liquid jacket which can provide more precise temperature control (Ballard et al., 1994) with the optical path set to 7.96 m (±0.5%). For each of the 12 burdens, 256 interferograms were averaged to reduce noise. Gain ranging improved the signal-to-noise by amplifying the wings of the interferogram before digitization. The single-sided interferograms were zero-filled 2× and phase corrected using Mertz’s method (Mertz, 1967). Decadic absorbance spectra were calculated in the usual manner [−log (I/I<sub>0</sub>)] using the spectrum of the cell with just N<sub>2</sub> carrier gas for I<sub>0</sub>. The final data product is a spectrum that corresponds to an optical path of 1 m through a mixing ratio of 1 ppm<sub>v</sub> of analyte at 296 K.

For this particular molecule, several bands of interest were noted in the near-infrared (NIR) range, so 17 additional burdens were measured with alternate hardware optimized to improve the NIR signal/noise. These included a tungsten halide source, a Si/CaF<sub>2</sub> beamsplitter, and a photovoltaic InSb detector. The mirror scan speed was adjusted to 20 kHz, but all other collection parameters were as for the mid-infrared measurements (Sharpe et al., 2004). The NIR spectra covered the 1900 to 10 000 cm<sup>−1</sup> range, for a total range of 550–10 000 cm<sup>−1</sup>. Data are only plotted to 6500 cm<sup>−1</sup> as the few bands at higher frequencies are relatively weak. The FT-Raman spectra were collected over the range from 50 to 3600 cm<sup>−1</sup> Stokes shift and from −100 to −1000 cm<sup>−1</sup> anti-Stokes shift using a previously described instrument (Williams et al., 2006). Ra-

<sup>1</sup> Johnson, T. J., Sharpe, S. W., and Covert, M. A.: A Method for Quantitative Dissemination of Vapors, Rev. Sci. Instr., to be submitted, 2006.

man frequencies are calibrated using the interferometer HeNe laser and the Raman Nd:YAG laser. For a given FT-Raman spectrum the frequency accuracy has been shown to be better than  $1\text{ cm}^{-1}$ . Data collection parameters and methods for the high resolution IR spectra ( $0.0015\text{ cm}^{-1}$ ), including for peak positions reported in the far-infrared, have already been reported by Maki et al. (2001). Theoretical calculations of vibrational frequencies and infrared line intensities (peak maxima) were calculated using the NWChem software algorithm (Kendall et al., 2000). This ab initio method uses MP2 and was used with the largest basis set (6–311 g\*\*) possible that delivers both frequencies and intensities; the frequencies are typically too large, and are customarily scaled by a factor of 0.955 (Marshall et al., 2005). Other workers have very recently reported calculated frequencies, but not intensities, for  $\text{CH}_2\text{I}_2$  (Marshall et al., 2005). Although calculated at a higher level, there is good agreement with the present results.

### 3. Results

Figure 1 reports the quantitative gas-phase infrared spectrum<sup>2</sup> of methylene iodide (diiodomethane) from 550 to  $6500\text{ cm}^{-1}$ . The y-axis is quantitative such that the absorbance values correspond to an optical path of 1 m through a concentration of 1 ppm<sub>v</sub> of analyte at 296 K and 1 atm total pressure. The reported spectrum represents the weighted average of 12 individual measurements for the mid-infrared and 17 measurements for the near-infrared. The concatenated spectrum has been broken into four separate plots for visual clarity. Note that the plot in Fig. 1a has a different ordinate scale as the  $\nu_9$  band at  $584.21\text{ cm}^{-1}$  and the  $\nu_8$  band at  $1113.87\text{ cm}^{-1}$  are both IR-allowed fundamentals and are very intense bands. Plots 1b, 1c and 1d are all on the same scale, and all plots represent an average from multiple burdens of  $\text{CH}_2\text{I}_2$ , each burden pressure-broadened to 760 Torr. The peak positions and band types of the fundamentals for the present vapor-phase data are given in Table 1. Also in Table 1

<sup>2</sup>The  $\text{CH}_2\text{I}_2$  spectrum and other NWIR data can be found at <http://nwir.pnl.gov>.

## Quantitative $\text{CH}_2\text{I}_2$ vapor spectrum

T. J. Johnson et al.

Title Page

Abstract

Introduction

Conclusions

References

Tables

Figures

◀

▶

◀

▶

Back

Close

Full Screen / Esc

Print Version

Interactive Discussion

are the corresponding liquid-phase values, both infrared and Raman, as well as the vibrational assignments. Table 2 presents the integrated vapor-phase band strengths (in units of  $\text{cm}^{-1} \text{cm}^2 \text{molecule}^{-1}$ , or  $\text{cm molecule}^{-1}$ ) for the fundamentals. While the data in the NWIR database use base 10 logarithms, the band integrals in Table 2 use Naperian (natural) logarithms at 296 K for the peak height as the more common unit for S. Also in Table 2 are the frequencies and intensities as calculated by the ab initio program NWChem. As these are the first Fourier-transform measurements of vapor phase  $\text{CH}_2\text{I}_2$  the accuracy along the wavelength axis is much higher (Sharpe et al., 2004; Maki and Wells, 1991). High resolution vapor-phase infrared spectra confirm our low resolution estimates for many of the band origins given in Table 1. However, precise determination of the band origins can only be achieved through analysis of the high resolution data. Consequently, an error of  $\pm 0.1 \text{ cm}^{-1}$  should be assumed for all values given in Table 1 for the vapor phase spectra.

The Raman spectra aided in the assignment and confirmation of many vibrational bands, especially the polarized Raman spectra which helped to confirm assignment of vibrational modes with  $a_1$  symmetry (i.e. symmetric modes). The vibrational assignments largely agree with those of Voelz and co-workers (1953) as well as Ford (1975). The nine fundamentals in the  $\text{C}_{2v}$  point group are printed in bold in Table 1. The long path gas cell and greater instrumental sensitivity allow for observation of even very weak fundamentals including  $\nu_3$  ( $a_1$  symmetry,  $493.01 \text{ cm}^{-1}$ )  $\nu_7$  ( $b_1$ ,  $718.08 \text{ cm}^{-1}$ ) and  $\nu_2$  ( $a_1$ ,  $1373.61 \text{ cm}^{-1}$ ). The symmetric  $\nu_1$  ( $3002.00$ ),  $\nu_2$  ( $1373.61$ ),  $\nu_3$  ( $493.01$ ) and  $\nu_4$  ( $122 \text{ cm}^{-1}$ )  $a_1$  modes are easily assigned due their medium to very strong Raman signals which are all strongly polarized (i.e.  $a_1$  modes). We note that the  $\nu_4$  ( $122 \text{ cm}^{-1}$ ) fundamental was not observed in any of the IR gas-phase spectra, including path lengths  $> 35 \text{ m}$ . This diminished intensity does agree with that predicted by the ab initio calculations (Table 2). The  $\nu_8$  ( $1113.87$ ) and  $\nu_9$  ( $584.21$ ) IR bands are both  $b_2$  modes and dominate the IR spectrum. Although both appear to have B-type bands in the pressure-broadened  $0.1 \text{ cm}^{-1}$  measurements, high resolution ( $0.0015 \text{ cm}^{-1}$ ) measurements at low pressure do show A-type contours, and centralized Q-branch features as

## Quantitative $\text{CH}_2\text{I}_2$ vapor spectrum

T. J. Johnson et al.

Title Page

Abstract

Introduction

Conclusions

References

Tables

Figures

◀

▶

◀

▶

Back

Close

Full Screen / Esc

Print Version

Interactive Discussion



expected.

The  $\nu_5$  ( $a_2$ ) fundamental is seen in both the liquid Raman and liquid IR spectra at  $1033\text{ cm}^{-1}$ . As an  $a_2$  mode, it is IR forbidden in the  $C_{2v}$  point group, but we can tentatively assign the very weak  $1041.99\text{ cm}^{-1}$  band as the corresponding gas phase fundamental which has modest intensity in the liquid due to condensed phase interactions. The depolarized Raman signal helps assign the symmetry. The  $\nu_3 + \nu_9$  combination band is seen only in the gas phase at  $1075.04\text{ cm}^{-1}$ , while the band at  $2075.67$  is the  $\nu_2 + \nu_7$  combination. Many of the overtone, combination and difference bands are assigned for the first time. In particular, we assign for the first time many of the bands at frequencies  $>3500\text{ cm}^{-1}$ . Although these frequencies are outside the Raman spectrum, the vapor-phase band profiles (Fig. 2), along with the NWChem ab initio calculations make the assignments straightforward in most cases.

In terms of band strengths, the  $b_2 \nu_9$  ( $584.21\text{ cm}^{-1}$ ) and  $\nu_8$  ( $1113.87\text{ cm}^{-1}$ ) are clearly the most intense IR bands and dominate the spectrum. Both are pressure broadened at 760 Torr (Nitrogen) to form unresolved bands that are B-type in appearance but in fact are A-type; of the two,  $\nu_8$  is the more intense with a width (FWHM) of  $11.8\text{ cm}^{-1}$  and a peak amplitude  $1.2 \times 10^{-3}$  absorbance for 1 ppm-m. The spacing of the  $\text{CH}_2\text{I}_2$  rotational lines in the  $\nu_8$  and  $\nu_9$  bands is quite small and these do not resolve at atmospheric pressure. They do resolve at low pressure, however, and a high resolution study investigating and assigning both these bands is currently under way in our laboratory using previously described high resolution instrumentation (Maki et al., 2001).

For the remaining of the pressure-broadened bands shown in Fig. 1, many are of approximately the same band strength, and of these several are C-type bands that exhibit resolved Q-branches. We focus on these in particular, since the resolved structure better lends itself to open path monitoring, either via methods such as DOAS (Platt, 1994; Volkamer et al., 2005) or laser-based techniques. Three of these bands with the C-type profile will be considered in more detail for pressure-broadened (ambient) monitoring. Figure 2's top trace displays the  $\nu_1$  fundamental at  $3002.00\text{ cm}^{-1}$  along with the C-type  $\nu_6$  band at  $3073.01\text{ cm}^{-1}$ , where the plot again represents an optical

## Quantitative $\text{CH}_2\text{I}_2$ vapor spectrum

T. J. Johnson et al.

Title Page

Abstract

Introduction

Conclusions

References

Tables

Figures

◀

▶

◀

▶

Back

Close

Full Screen / Esc

Print Version

Interactive Discussion

depth of 1 ppm-m. For the  $\nu_6$  band the Q-branch has a peak height of  $2.65 \times 10^{-5}$  OD with a Q-branch differential peak height of  $1.98 \times 10^{-5}$ . The middle trace of Fig. 2 plots the  $\nu_2 + \nu_6$  combination band at  $4426.52 \text{ cm}^{-1}$ , and the lower trace shows the  $2\nu_1$  overtone at  $5921.62 \text{ cm}^{-1}$  along with the  $(\nu_1 + \nu_6)$  combination C-type band at  $5953.31 \text{ cm}^{-1}$ .

Note that the y-axis has been held the same in the three plots to show the relative line strengths, most of which are comparable, though all these bands are approximately two orders of magnitude weaker than  $\nu_8$  or  $\nu_9$  in the long-wave infrared.

#### 4. Discussion

Both the intense IR fundamentals,  $\nu_9$  at  $584.21 \text{ cm}^{-1}$  and  $\nu_8$  at  $1113.87 \text{ cm}^{-1}$ , shown in Fig. 1 are in fact unresolved A-type bands and fall in an “atmospheric window”. For low resolution monitoring the  $\nu_8$  band at  $1113.87 \text{ cm}^{-1}$  is the most promising as it lies in the center of the LWIR window. We note that both the  $\nu_8$  and  $\nu_9$  fundamentals are of  $b_2$  symmetry in the  $C_{2v}$  point group. At  $0.1 \text{ cm}^{-1}$  resolution both appear as B-type bands, but very high resolution spectra recorded at low pressure have shown the expected A-type structure. The  $\nu_8$  band has a width (FWHM) of  $11.8 \text{ cm}^{-1}$ , and a peak amplitude of  $1.2 \times 10^{-3}$  OD for 1 ppm-m. At lower resolution, typically 4 or  $8 \text{ cm}^{-1}$ , used in most ambient monitoring situations with an active or semi-active FTIR system (Johnson et al., 2004), the one minute detection limits are of the order  $10^{-4}$  OD (Griffith and Jamie, 2000). This suggests that for a 500 m (open) path, an optimistic detection limit for  $\text{CH}_2\text{I}_2$  is 500 ppt<sub>v</sub>. Consequently, current FT-methods would be challenged to observe the anticipated <100 ppt<sub>v</sub> biogenic levels of  $\text{CH}_2\text{I}_2$  (Carpenter et al., 1999). Although they are the strongest bands, the  $\nu_8$  and  $\nu_9$  bands are unresolved at 760 Torr and may not be of use for open-path laser monitoring. As mentioned above, however, these bands do resolve at low pressure, and their assignments and potential for monitoring will be discussed in a separate work. We are optimistic that the line strengths are of sufficient intensity to be useful for extractive monitoring, e.g. using Pb-salt or QC-laser

Title Page

Abstract

Introduction

Conclusions

References

Tables

Figures

◀

▶

◀

▶

Back

Close

Full Screen / Esc

Print Version

Interactive Discussion

systems.

Of the laser methods, Pb-salt laser systems have been used extensively in the mid-IR ( $\lambda=3$  to  $20\text{ }\mu\text{m}$ ) albeit almost exclusively as point sensors using long path cells at low pressure. Several near-IR laser systems have been deployed using techniques such as FM modulation (Johnson et al., 1991b) or cavity ring-down methods (Bitter et al., 2005). Until recently, the greatest limitations appear to be the tunability and wavelength availability of the lasers, predominantly limited to the wavelengths used by the telecommunications industry (e.g.  $1.3$  or  $1.55\text{ }\mu\text{m}$ ). The recent advent of quantum cascade (QC) lasers shows excellent promise as these are available from the near-IR to the terahertz (THz) wavelengths. These lasers have also demonstrated an important feature in that they have significant tuning ranges, typically  $>0.5\%$  or more of the central wavelength, depending on the nature of the device fabrication. This allows, for example, tuning across a  $1\text{ cm}^{-1}$  wide Q-branch for atmospheric monitoring purposes.

Figure 3 demonstrates one possibility for atmospheric monitoring using the Q-branch of the  $760\text{ Torr } \nu_6$  band at  $3073.01\text{ cm}^{-1}$  ( $3.25\text{ }\mu\text{m}$ ); this  $\text{CH}_2\text{I}_2$  spectrum ( $1\text{ ppm-m}$ ) is plotted in pink. Also plotted in Fig. 3 are typical expected ambient concentrations (Warneck, 1988) of  $1.8\text{ ppm}$  for methane (green) and the optical density corresponding to  $10\text{ Torr}$  of  $\text{H}_2\text{O}$  (blue). The water data were taken from the HITRAN database (Rothman et al., 2005) since the HITRAN calculated data have no noise that can obfuscate the signal when expanded thousands of times. The database was examined for other potential interferents with high background concentrations (e.g.  $\text{N}_2\text{O}$ ,  $\text{CO}_2$ ,  $\text{CO}$ ), but these did not show any interfering absorptions at these wavelengths. The Q-branch at  $3073\text{ cm}^{-1}$  corresponds to a differential peak height of  $1.98\times 10^{-5}$  OD for  $1\text{ ppm-m}$ , which is also equivalent to  $1.98\times 10^{-5}$  for  $1\text{ ppb-km}$ . The  $3.25\text{ }\mu\text{m}$  wavelength can be accessed by both Pb-salt and quantum cascade diode lasers. Assuming an open path laser-based system with a  $10\text{ km}$  path length, in order to achieve a  $50\text{ ppt}_v$  detection limit, a spectrometer would need a detection sensitivity corresponding to  $\sim 1\times 10^{-5}$  OD or better. For an extractive laser-based system with a  $200\text{ m}$  path length, in order to achieve a  $50\text{ ppt}_v$  detection limit, a spectrometer would need a detection sensitivity cor-

## Quantitative $\text{CH}_2\text{I}_2$ vapor spectrum

T. J. Johnson et al.

Title Page

Abstract

Introduction

Conclusions

References

Tables

Figures

◀

▶

◀

▶

Back

Close

Full Screen / Esc

Print Version

Interactive Discussion

responding to  $\sim 2 \times 10^{-7}$  OD or better at these wavelengths. Although such a measurement would pose a challenge, the best extractive measurements at these wavelengths are now achieving such detection limits using difference frequency generation (Richter et al., 2002) or improved Pb-salt diode laser systems (Wert et al., 2003; Schiller et al., 2001). The weak methane lines near  $3073 \text{ cm}^{-1}$  pose a concern, but the  $\text{CH}_4$  mixing ratios can be expected to be low and constant in marine atmospheres. It is also possible that using an extractive system with a near-infrared detector (e.g. InSb) and a long path cell that some of the lines in the Q-branch resolve and separate from those of methane, also possibly increasing the depth of any one of the  $\text{CH}_2\text{I}_2$  lines. Very recent results have shown that the  $\nu_1$  and  $\nu_6$  bands near  $3.3 \mu\text{m}$  do resolve at low pressure and may also be useful for atmospheric monitoring (Orphal and Ibrahim, 2005).

Figure 4 plots the  $(\nu_2 + \nu_6)$  combination band at  $4426.52 \text{ cm}^{-1}$  which we report for the first time. Figure 4's bottom trace shows some of the sharp lines of the  $2\nu_1$  overtone band of hydrogen iodide gas, HI. It was hoped that using a single laser it may be possible to monitor simultaneously both HI and  $\text{CH}_2\text{I}_2$  by slight tuning of the wavelength. However, closer inspection of the database immediately showed that expected concentrations of 1.8 ppmv of  $\text{CH}_4$  or 316 ppbv of nitrous oxide (Evans and Puckrin, 1997) would interfere with such a measurement, particularly the  $\text{N}_2\text{O}$ . However, extractive measurements may still afford a practical separation of the HI/ $\text{CH}_2\text{I}_2$  pair from the interfering signals, particularly at wavenumbers  $> 4440 \text{ cm}^{-1}$ , although wall adhesion mechanisms are of concern for species such as HI, HCl, or  $\text{HNO}_3$  (Chackerian et al., 2003; Johnson et al., 2003).

The traces in Fig. 5 display two new bands of  $\text{CH}_2\text{I}_2$ , namely the  $2\nu_1$  overtone ( $A_1$  symmetry, B-type) at  $5921.62 \text{ cm}^{-1}$ , as well as the  $(\nu_1 + \nu_6)$  combination C-type band at  $5953.31 \text{ cm}^{-1}$ . Both have resolved rotational structure even when pressure broadened to one atmosphere. The structure in these bands suggests the possibility of remote sensing as the Q-branch at  $5953 \text{ cm}^{-1}$  as well as several of the individual rotational lines, e.g. in the  $2\nu_1$  R branch near  $5930 \text{ cm}^{-1}$  have differential absorbances of  $\sim 3 \times 10^{-6}$ . Such structure is very helpful not only for laser monitoring, but also for DOAS

## Quantitative $\text{CH}_2\text{I}_2$ vapor spectrum

T. J. Johnson et al.

Title Page

Abstract

Introduction

Conclusions

References

Tables

Figures

◀

▶

◀

▶

Back

Close

Full Screen / Esc

Print Version

Interactive Discussion

methods, which have been used to monitor trace gases such as HONO at the (sub-) ppbv levels (Platt et al., 1980). Detection limits of  $10^{-4}$  are achievable, and path lengths of  $>10$  km are now common. In a much related work Alicke and co-workers (1999) have recently used such a set-up in the UV-visible with a 14.6 km path to measure IO at levels of  $<10$  ppt<sub>v</sub>. For the case of CH<sub>2</sub>I<sub>2</sub>, if one assumes a 15 km (e.g. estuary) path and a differential cross section of  $3 \times 10^{-6}$  ppm-m (equivalent to  $2.8 \times 10^{-21}$  cm<sup>2</sup>/molecule base-e) in order to observe 100 ppt<sub>v</sub> of CH<sub>2</sub>I<sub>2</sub> it would be necessary to detect an absorbance of  $4.5 \times 10^{-6}$  at these wavelengths. This is certainly a challenging detection limit, but DOAS detection for methane has recently been reported at these wavelengths (Frankenberg et al., 2005).

Of the CH<sub>2</sub>I<sub>2</sub> near-infrared bands discussed above, several fortuitously display resolved structure, even when broadened to 1 atmosphere. Although the telecommunications diode lasers are limited in wavelength selection, several recent technologies offer methods for sensitive trace gas detection using such lines (bands). These include tunable optical parametric oscillators (OPOs), difference frequency generation (DFG, Richter et al., 2002) and, recently, red-shifting the emission wavelength of near-IR lasers via high pressures (Adamiec et al., 2004). In terms of the CH<sub>2</sub>I<sub>2</sub> photochemistry in the presence of ozone, it may be possible to monitor the CH<sub>2</sub>I<sub>2</sub>, HI and IO simultaneously in a chamber type experiment as suggested by Mäkelä et al. (2002). The  $\nu_6$  3073 cm<sup>-1</sup> band may be useful in laboratory experiments where CH<sub>4</sub> and H<sub>2</sub>O concentrations are reduced. Also, monitoring at 3  $\mu$ m offers the advantage of less light scattering compared to visible or NIR regions.

## 5. Summary

The quantitative infrared and near-infrared vapor-phase spectra of diiodomethane, CH<sub>2</sub>I<sub>2</sub>, have been reported for the first time. Using FT-IR, FT-Raman spectroscopy and ab initio computational methods we have completed a vibrational assignment. The atmospherically broadened spectra exhibit C-type bands near 5953, 4426 and

## Quantitative CH<sub>2</sub>I<sub>2</sub> vapor spectrum

T. J. Johnson et al.

Title Page

Abstract

Introduction

Conclusions

References

Tables

Figures

◀

▶

◀

▶

Back

Close

Full Screen / Esc

Print Version

Interactive Discussion

3073 cm<sup>-1</sup>, all having resolved rotational structure, including Q-branches with widths of ~1 cm<sup>-1</sup>. These could be potentially useful for atmospheric monitoring of this important species. There are also two very strong b<sub>2</sub> A-type bands (appearing as B-type), ν<sub>9</sub> at 584.21 cm<sup>-1</sup> and ν<sub>8</sub> at 1113.87 cm<sup>-1</sup> that do not resolve at atmospheric pressure. It is hoped that at low pressure the resolved lines may be useful for extractive monitoring. These investigations are currently in progress.

*Acknowledgements.* PNNL is operated for the US Department of Energy by the Battelle Memorial Institute under contract DE-AC06-76RLO 1830. This work was supported under the DOE NA-22 program and we gratefully acknowledge that support. The experiment and calculations were performed at the W. R. Wiley Environmental Molecular Sciences Laboratory, a national scientific user facility sponsored by DOE's Office of Biological and Environmental Research and located at Pacific Northwest National Laboratory, which is operated for DOE by Battelle.

## References

- Adamiec, P., Salhi, A., Bohdan, R., Bercha, A., Dybala, F., Trzeciakowski, W., Rouillard Y., and Joullié, A.: Pressure-tuned InGaAsSb/AlGaAsSb Diode Laser with 700 nm Tuning Range, Appl. Phys. Lett., 85(19), 4292–4294, 2004.
- Alicke, B., Hebestreit, K., Stutz J., and Platt, U.: Iodine Oxide in the Marine Boundary Layer, Nature, 397, 572–573, 1999.
- Ballard, J., Strong, K., Remedios, J. J., Page, M., and Johnston, W. B.: A Coolable Long Path Absorption Cell for Laboratory Spectroscopic Study of Gases, J. Quant. Spectrosc. Rad. Transf., 52, 677–691, 1994.
- Bertie, J. E.: Specification of Components, Methods and Parameters in Fourier Transform Spectroscopy by Michelson and Related Interferometers, Pure and Appl. Chem., 70(10), 2039, 1998.
- Birk, M., Hausamann, D., Wagner G., and Johns, J. W.: Determination of Line Strengths by Fourier-transform Spectroscopy, Appl. Opt., 35, 2971–2985, 1996.
- Bitter, M., Ball, S. M., Povey, I. M., and Jones, R. L.: A Broadband Cavity Ringdown Spectrometer for in situ Measurement of Atmospheric Trace Gases, Atmos. Chem. Phys., 5, 2547–2560,

## Quantitative CH<sub>2</sub>I<sub>2</sub> vapor spectrum

T. J. Johnson et al.

Title Page

Abstract

Introduction

Conclusions

References

Tables

Figures

◀

▶

◀

▶

Back

Close

Full Screen / Esc

Print Version

Interactive Discussion

2005,

SRef-ID: 1680-7324/acp/2005-5-2547.

Burkholder, J. B., Curtius, J., Ravishankara, A. R., and Lovejoy, E. R.: Laboratory Studies of the Homogeneous Nucleation of Iodine Oxide, *Atmos. Chem. Phys.*, 4, 19–34, 2004,

SRef-ID: 1680-7324/acp/2004-4-19.

Carpenter, L. J., Sturges, W. T., Penkett, S. A., Liss, P. S., Alicke, B., Hebestreit K., and Platt, U.: Short-lived Alkyl Iodides and Bromides at Mace Head, Ireland: Links to Biogenic Sources and Halogen Oxide Production, *J. Geophys. Res.*, 104 (D1), 1679–1689, 1999.

Chackerian, C., Sharpe, S. W., and Blake, T. A.: Anhydrous Nitric Acid Integrated Cross Sections: 820–5300 cm<sup>-1</sup>, *J. Quant. Spectr. Rad. Transf.*, 82(1–4): 429–441, 2003.

Chameides, W. L. and Davis, D. D.: Iodine: Its Possible Role in Tropospheric Photochemistry, *J. Geophys. Res.*, C, 85, 7383–7398, 1980.

Chase, D. B.: Nonlinear Detector Response and FT-IR, *Appl. Spec.*, 38(4), 491–494, 1984.

Chu, P. M., Guenther, F. R., Rhoderick, G. C., and Lafferty, W. J.: The NIST Quantitative Infrared Database, *J. Res. Natl. Inst. Stand. Technol.*, 104, 59, 1999.

Cox, R. A., Bloss, W. J., Jones, R. L., and Rowley, D. M.: OIO and the Atmospheric Cycle of Iodine, *Geophys. Res. Lett.*, 26(13), 1857–1860, 1999.

Evans, W. F. J. and Puckrin, E.: A Wintertime Measurement of the Greenhouse Radiation from Nitrous Oxide, *Can. J. Atmos. Sciences and Spectr.*, 42(5), 141–145, 1997.

Ford, T. A.: Infrared and Raman Spectra and Vibrational Assignments of Diiodomethane and Its Deuterated Analogs, *J. Mol. Spec.*, 58, 185–193, 1975.

Frankenberg, C., Meirink, J. F., van Weele, M., Platt, U., and Wagner, T.: Assessing Methane Emissions from Global Space-Borne Observations, *Science*, 308, 1010–1014, 2005.

Gilles, M. K., Turnipseed, A. A., Burkholder, J. B., Ravishankara, A. R., and Solomon, S.: Kinetics of the IO radical: 2. Reaction of IO with BrO, *J. Phys. Chem. A*, 101, 5526–5534, 1997.

Griffith, D. W. T. and Jamie, I. M.: Fourier Transform Infrared Spectrometry in Atmospheric and Trace Gas Analysis, in: *Encyclopedia of Analytical Chemistry*, edited by: Meyers, R. A., 1979–2000, 2000.

Harwood, M. H., Burkholder, J. B., Hunter, M., Fox, R. W., and Ravishankara, A. R.: Absorption Cross Sections and Self-reaction Kinetics of the IO radical, *J. Phys. Chem. A*, 101, 853–863, 1997.

Henry, B. R. and Hung, I.-F.: Mass Effects on the Applicability of local Mode Description of the

ACPD

6, 1275–1299, 2006

## Quantitative CH<sub>2</sub>I<sub>2</sub> vapor spectrum

T. J. Johnson et al.

Title Page

Abstract

Introduction

Conclusions

References

Tables

Figures

◀

▶

◀

▶

Back

Close

Full Screen / Esc

Print Version

Interactive Discussion

EGU



High Energy Overtone Spectra of Difluoro-, Dichloro-, Dibromo- and Diiodomethane, Chem. Phys., 29, 465–475, 1978.

Hoffmann, T., O'Dowd, C. D., and Seinfeld, J. H.: Iodine oxide homogeneous Nucleation: An Explanation for Coastal New Particle Production, Geophys. Res. Lett., 28(10), 1949–1952, 2001.

Jimenez, J. L., Bahreini, R., Cocker III, D. R., Zhuang, H., Varutbangkul, V., Flagan, R. C., Seinfeld, J. H., O'Dowd, C. D., and Hoffman, T.: New Particle Formation from Photooxidation of Diiodomethane, J. Geophys. Res. D, 108, D10, 4318–4343, 2003.

Johnson, T. J., Roberts, B. A., and Kelly, J. F.: Semiactive Infrared Remote Sensing: A Practical Prototype and Field Comparison, Appl. Opt., 43(3), 638–650, 2004.

Johnson, T. J., Wienhold, F. G., Burrows, J. P., and Harris, G. W.: Frequency Modulation Spectroscopy at 1.3  $\mu\text{m}$  Using InGaAsP Lasers: A Prototype Field Instrument for Atmospheric Chemistry Research, Appl. Opt., 30, 407–413, 1991a.

Johnson, T. J., Wienhold, F. G., Burrows, J. P., Harris, G. W., and Burkhard, H.: Measurements of Line Strengths in the  $\text{HO}_2\nu_1$  Overtone Band at 1.5  $\mu\text{m}$  Using an InGaAsP Laser, J. Phys. Chem., 95, 6499–6502, 1991b.

Johnson, T. J., Valentine, N. B., and Sharpe, S. W.: Mid-infrared versus Far-infrared (THz) Relative Intensities of Room-temperature *Bacillus* spores, Chem. Phys. Lett., 403, 152–157, 2005.

Johnson, T. J., Sams, R. L., Blake, T. A., Sharpe, S. W., and Chu, P. M.: Removing Aperture-Induced Artifacts from FTIR Intensity Values, Appl. Opt. 41, 2831–2839, 2002.

Johnson, T. J., Disselkamp, R. S., Su, Y.-F., Fellows, R. J., Alexander, M. L., and Driver, C. L.: Gas-phase Hydrolysis of  $\text{SOCl}_2$ : Implications for Its Atmospheric Fate, J. Phys. Chem. A, 107(32), 6183–6190, 2003.

Kasper, J. V. V., Parker, J. H., and Pimentel, G. C.: Atomic Iodine Photodissociation Laser, Appl. Phys. Lett., 5(11), 231–233, 1964.

Kasper, J. V. V., Parker, J. H., and Pimentel, G. C.: Iodine-Atom Laser Emission in Alkyl Iodine Photolysis, J. Chem. Phys., 43, 1827–1828, 1965.

Kendall, R. A., Apra, E., Bernholdt, D. E., Bylaska, E. J., Dupuis, M., Fann, G. I., Harrison, R. J., Ju, J., Nichols, J. A., Nieplocha, J., Straatsma, T. P., Windus, T. L., and Wong, A. T.: High Performance Computational Chemistry: An Overview of NWChem, a Distributed Parallel Application, Computer Phys. Comm., 128, 260–283, 2000.

Kolb, C. E.: Iodine's Air of Importance, Nature, 417, 597–598, 2002.

ACPD

6, 1275–1299, 2006

## Quantitative $\text{CH}_2\text{I}_2$ vapor spectrum

T. J. Johnson et al.

Title Page

Abstract

Introduction

Conclusions

References

Tables

Figures

◀

▶

◀

▶

Back

Close

Full Screen / Esc

Print Version

Interactive Discussion

EGU



- Kroger, P. M., Demou, P. C., and Riley, S. J.: Polyhalide Photofragment Spectra. I. Two-photon Two-step Photodissociation of Methylene Iodide, *J. Chem. Phys.*, 65(5), 1823–1834, 1976.
- Mäkelä, J. M., Hoffmann, T., Holzke, C., Väkevää, M., Suni, T., Mattila, T., Aalto, P. P., Tapper, U., Kauppinen, E. I., and O'Dowd, C. D.: Biogenic Iodine Emissions and Identification of End-products in Coastal Ultrafine Particles During Nucleation Bursts, *J. Geophys. Res.*, 107(D19), 8110–8124, 2002.
- Maki, A., Blake, T. A., Sams, R. L., Vulpanovici, N., Barber, J., Chrysostom, E. T. H., Masiello, T., Nibler, J. W., and Weber, A.: *J. Mol. Spectrosc.*, 210, 240–249, 2001.
- Maki, A. G. and Wells, J. S.: Wavenumber Calibration Tables from Heterodyne Frequency Measurements, NIST Special Publication 821, National Institute of Standards and Technology, U.S. Government Printing Office, Washington, D.C., 1991.
- Marshall, P., Srinivas, G. N., and Schwartz, M.: *J. Phys. Chem. A*, 109, 6371–6379, 2005.
- McFiggans, G., Coe, H., Burgess, R., Allen, J., Cubison, M., Alfarra, M. R., Saunders, R., Saiz-Lopez, A., Plane, J. M. C., Wevill, D. J., Carpenter, L. J., Rickard, A. R., and Monks, P. S.: Direct Evidence for Coastal Iodine Particles from Laminaria Macroalgae – Linkage to Emissions of Molecular Iodine, *Atmos. Chem. Phys.*, 4, 701–713, 2004, [SRef-ID: 1680-7324/acp/2004-4-701](#).
- Mertz, L.: Auxiliary Computation for Fourier Spectrometry, *Infr. Phys.*, 7, 17, 1967.
- Orphal, J. and Ibrahim, N.: The  $\nu_1$  and  $\nu_6$  Bands of Diiodomethane,  $\text{CH}_2\text{I}_2$ , around 3.3. Microns Studied by High-Resolution Fourier-Transform Spectroscopy, in: 19th Colloquium on High Resolution Molecular Spectroscopy, Salamanca, Spain, 11–16 September, 2005.
- Platt, U.: Differential Optical Absorption Spectroscopy, in: *Monitoring by Spectroscopic Techniques*, edited by: Sigrist, M. W., chapter 2, 27–84, Wiley & Sons, New York, 1994.
- Platt, U., Perner, D., Harris, G. W., Winer, A. M., and Pitts, J. N.: Observations of Nitrous Acid in an Urban Atmosphere by Differential Optical-Absorption, *Nature*, 285, 312–314, 1980.
- Richter, D., Fried, A., Wert, B. P., Walega, J. G., and Tittel, F. K.: Development of a Tunable mid-IR Difference Frequency Laser Source for Highly Sensitive Airborne Trace Gas Detection, *Appl. Phys. B*, 75, 281–288, 2002.
- Rothman, L. S., Jacquemart, D., Barbe, A., Brenner, D. C., et al.: The HITRAN 2004 Molecular Spectroscopic Database, *J. Quant. Spectrosc. Rad. Transf.*, 96, 139–204, 2005.
- Schiller, C. L., Locquiao, S., Johnson, T. J., and Harris, G. W.: Atmospheric Measurements of HONO by Tunable Diode Laser Absorption Spectroscopy, *J. Atmos. Chem.*, 40, 275–293, 2001.

## Quantitative $\text{CH}_2\text{I}_2$ vapor spectrum

T. J. Johnson et al.

Title Page

Abstract

Introduction

Conclusions

References

Tables

Figures

◀

▶

◀

▶

Back

Close

Full Screen / Esc

Print Version

Interactive Discussion

- Schmitt, G. and Comes, F. J.: Spectroscopic Investigations of the Photolysis of Diiodomethane, *J. Mol. Struct.*, 61, 51–54, 1980.
- Sharpe, S. W., Kelly, J. F., Hartman, J. S., Gmachl, C., Capasso, F., Sivco, D. L., Baillargeon, J. N., and Cho, A. Y.: High-resolution (Doppler-limited) Spectroscopy Using Quantum-cascade Distributed-feedback Lasers, *Opt. Lett.*, 23(17), 1396–1398, 1998.
- Sharpe, S. W., Johnson, T. J., Chu, P. M., Kleimeyer J., and Rowland, B.: Quantitative Infrared Spectra of Vapor Phase Chemical Agents, *SPIE Proceedings*, 5058, 19–27, 2003.
- Sharpe, S. W., Johnson, T. J., Sams, R. L., Chu, P. M., Rhoderick, G. C., and Johnson, P. A.: Gas-phase Databases for Quantitative Infrared Spectroscopy, *Appl. Spectr.*, 58(12), 1452–1461, 2004.
- Solomon, S., Garcia, R. R., and Ravishankara, A. R.: On the Role of Iodine in Ozone Depletion, *J. Geophys. Res.*, 99(D10), 20 491–20 499, 1994.
- Voelz, F. L., Cleveland, F., Meister, A. G., and Bernstein, R. B.: Substituted Methanes. XVII: Vibrational Spectra, Potential Constants, and Calculated Thermodynamic Properties of Diiodomethane, *J. Opt. Soc. Am.*, 43, 1061–1064, 1953.
- Vogt, R., Sander, R., von Glasow, R., and Crutzen, P. J.: Iodine Chemistry and Its Role in Halogen Activation and Ozone Loss in the Marine Boundary Layer, *J. Atmos. Chem.*, 32, 375–395, 1999.
- Volkamer, R., Molina, L. T., Molina, M. J., Shirley, T., and Brune, W. H.: DOAS Measurement of Glyoxal as an Indicator for Fast VOC Chemistry in Urban Air, *Geophys. Res. Lett.*, 32, L08806 doi:10.1029/2005GL022616, 2005.
- Warneck, P.: *Chemistry of the Natural Atmosphere*, p. 146 ff., Academic Press, San Diego, 1988.
- Wert, B. P., Fried, A., Rauenbuehler, S., Walega, J., and Henry, B.: Design and Performance of a Tunable Diode Laser Absorption Spectrometer for Airborne Formaldehyde Measurements, *J. Geophys. Res.*, 108(D12), 4350–4362, 2003.
- Williams, S. D., Johnson, T. J., Gibbons, T. P., and Kitchens, C. L.: Relative Raman Intensities in C<sub>6</sub>H<sub>6</sub>, C<sub>6</sub>D<sub>6</sub>, and C<sub>6</sub>F<sub>6</sub>: a Comparison of Different Computational Methods, *Theo. Chem. Acc.*, in press, 2005.

## Quantitative CH<sub>2</sub>I<sub>2</sub> vapor spectrum

T. J. Johnson et al.

Title Page

Abstract

Introduction

Conclusions

References

Tables

Figures

◀

▶

◀

▶

Back

Close

Full Screen / Esc

Print Version

Interactive Discussion

Quantitative CH<sub>2</sub>I<sub>2</sub>  
vapor spectrum

T. J. Johnson et al.

**Table 1.** Observed Raman (liquid), Infrared (liquid and gas) vibrational frequencies, Raman polarizations and (for vapor measurements) band types of CH<sub>2</sub>I<sub>2</sub>, together with symmetries and vibrational assignments. Frequencies are in cm<sup>-1</sup>. Fundamental frequencies are printed in bold. Details can be found in text. NS=not seen, OOR=out of range.

Ram Liq	Ram str	Ram Polz	IR Liq	Liq Str	IR Gas	Band Type Rel. Intens.	Assm't	SYM
<b>121</b>	<b>vs</b>	<b>pol</b>	<b>122</b>	<b>w</b>	<b>NS</b>		<b><math>\nu_4</math></b>	<b><math>a_1</math></b>
197	w	pol	NS	NS	NS			
238	w	pol	NS	NS	NS		$2\nu_4$	$A_1$
365	w	pol	NS	NS	NS		$\nu_3-\nu_4$	$A_1$
448	vw		448		463.79		$\nu_9-\nu_4$	
<b>486</b>	<b>vs</b>	<b>pol</b>	<b>485</b>	<b>w</b>	<b>493.01</b>	<b>B-vw</b>	<b><math>\nu_3</math></b>	<b><math>a_1</math></b>
<b>571</b>	<b>m</b>	<b>dp</b>	<b>571</b>	<b>s</b>	<b>584.21</b>	<b>A-vs</b>	<b><math>\nu_9</math></b>	<b><math>b_2</math></b>
604	w	pol	NS	NS			$\nu_3+\nu_4$	$A_1$
<b>717</b>	<b>w</b>	<b>dp</b>	<b>717</b>	<b>s</b>	<b>718.08</b>	<b>C</b>	<b><math>\nu_7</math></b>	<b><math>b_1</math></b>
851	w	?	851	vw	NS			
969	w	pol	NS	NS	NS		$2\nu_3$	$A_1$
<b>1032</b>	<b>w</b>	<b>dp</b>	<b>1033</b>	<b>w</b>	<b>1041.99</b>	<b>vw</b>	<b><math>\nu_5</math></b>	<b><math>a_2</math></b>
					1075.04	<b>vw</b>	$\nu_3+\nu_9$	$B_2$
<b>1109</b>	<b>m</b>	<b>dp</b>	<b>1106</b>	<b>vs</b>	<b>1113.87</b>	<b>A-vs</b>	<b><math>\nu_8</math></b>	<b><math>b_2</math></b>
1134	m	pol	NS	NS	NS	NS	$2\nu_9$	$A_1$
1181	vw		1181	w	1189.1	w	$\nu_3+\nu_7$	$B_1$
NS			1226	m	1229.42	A-s	$\nu_4+\nu_8$	$B_2$
<b>1353</b>	<b>m</b>	<b>pol</b>	<b>1352</b>	<b>m</b>	<b>1373.61</b>	<b>B-w</b>	<b><math>\nu_2</math></b>	<b><math>a_1</math></b>
1434	m	pol	NS	NS	NS		$2\nu_7$	$A_1$
?			1595	vw	1603.39	w	$\nu_3+\nu_8$	$B_2$
1672	w	pol	NS	NS	1714.86	C-w	$\nu_4+\nu_5+\nu_9$	$B_1$
1755	w	dp	NS	NS	1754	vw	$\nu_5+\nu_7$	$B_2$
NS			1837		1864.97	w	$\nu_7+2\nu_9$	$B_1$
NS			1921	w	1953.86	w	$\nu_2+\nu_9$	$B_2$
1995	vw	pol	NS	NS				
2058	w	dp	2056		2075.67	C	$\nu_2+\nu_7$	$B_1$
NS			2132		2142.42	C-s	$\nu_5+\nu_9$	$B_1$
2209	w	pol	2209		2222.42	B	$2\nu_8$	$A_1$
2238	w	pol	NS	NS	NS			$A_1$
2360	w	pol	NS	NS	NS			$A_1$
2453	w	dp	2454		2482.14	A	$\nu_2+\nu_8$	$B_2$
2504	vw		NS		NS		$\nu_2+2\nu_9$	$A_1$
NS		NS	2549	vw	2560.12	w	$\nu_2+\nu_3+\nu_7$	$B_1$
2602	m	pol	NS	NS	2631.70	vw	$2\nu_5+\nu_9$	$B_2$
<b>2967</b>	<b>vs</b>	<b>pol</b>	<b>2968</b>	<b>s</b>	<b>3002.00</b>	<b>B-s</b>	<b><math>\nu_1</math></b>	<b><math>a_1</math></b>
<b>3046</b>	<b>s</b>	<b>dp</b>	<b>3046</b>	<b>vs</b>	<b>3073.01</b>	<b>C-s</b>	<b><math>\nu_6</math></b>	<b><math>b_1</math></b>
3332	w	pol	NS	NS	3323.23	B-w		
3573	w	pol	NS	NS	3585.93	B-w	$\nu_1+\nu_9$	$B_2$
OOR			3757	m	3785.26	B-w	$\nu_6+\nu_7$	$A_1$
OOR			4061	m	4097.60	A/B-s	$\nu_5+\nu_6$	$B_2$
OOR			4377	m	4426.52	C-s	$\nu_2+\nu_6$	$B_1$
OOR			5852	w	5921.62	B-m	$2\nu_1$	$A_1$
OOR			5892	w	5953.31	C-m	$\nu_1+\nu_6$	$B_1$
OOR			6094	w	6102.68	B-m	$2\nu_6$	$A_1$

Title Page

Abstract

Introduction

Conclusions

References

Tables

Figures

◀

▶

◀

▶

Back

Close

Full Screen / Esc

Print Version

Interactive Discussion

# Quantitative CH<sub>2</sub>I<sub>2</sub> vapor spectrum

T. J. Johnson et al.

**Table 2.** Observed Raman (liquid) and infrared (liquid and gas) fundamental vibrational frequencies along with gas-phase band integrals for the fundamental vibrations of CH<sub>2</sub>I<sub>2</sub>. Frequencies are in cm<sup>-1</sup> and band integrals are in units of cm-molecule<sup>-1</sup>, using Napierian (natural) logarithms at 296 K for the peak heights, and have been multiplied by 10<sup>18</sup>. Also listed are the frequencies (scaled by 0.955) and intensities (relative to  $\nu_8$ ) as predicted by NWChem. Details in text.

Assm't	SYM	Ram Liq	IR Liq	IR Gas	Gas Bnd / limits	Band/ cm/molec 296 K×1e18	NWC Freq'y Adjusted	NWC Ints'y Rel to $\nu_8$
$\nu_4$	a <sub>1</sub>	121	122	NS	NS	NS	117	0.02
$\nu_3$	a <sub>1</sub>	486	485	493.01	NC	NC	476	0.15
$\nu_9$	b <sub>2</sub>	571	571	584.21	600–550	5.1240	579	28.60
$\nu_7$	b <sub>1</sub>	717	717	718.08	775–665	0.8785	705	9.02
$\nu_5$	a <sub>2</sub>	1032	1033	1041.99	1048–1031	0.0008	1045	–
$\nu_8$	b <sub>2</sub>	1109	1106	1113.87	1135–1090	13.0800	1135	100.00
$\nu_2$	a <sub>1</sub>	1353	1352	1373.61	1420–1330	0.0159	1366	0.16
$\nu_1$	a <sub>1</sub>	2967	2968	3002.00	3030–2950	0.0756	3030	0.26
$\nu_6$	b <sub>1</sub>	3046	3046	3073.01	3140–3030	0.4147	3111	2.80

Title Page

Abstract

Introduction

Conclusions

References

Tables

Figures

I◀

▶I

◀

▶

Back

Close

Full Screen / Esc

Print Version

Interactive Discussion

EGU

**Quantitative CH<sub>2</sub>I<sub>2</sub>  
vapor spectrum**

T. J. Johnson et al.

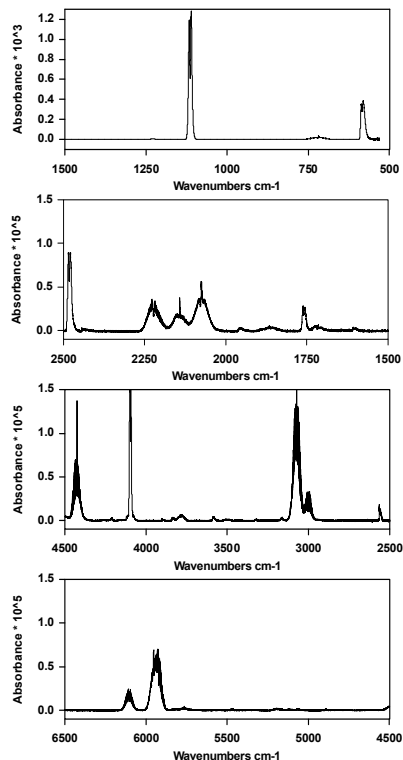


**Fig. 1.** Mid- and near-infrared quantitative spectrum of diiodomethane (CH<sub>2</sub>I<sub>2</sub>) from 6500 to 550 cm<sup>-1</sup>, recorded at 0.1 cm<sup>-1</sup> resolution. The spectrum is actually a composite derived from multiple spectra that corresponds to 1 ppm-m of gas at 296 K pressure-broadened to 760 Torr. Note that due to the strong bands at 584 and 1114 cm<sup>-1</sup> frame a has been multiplied by 10<sup>3</sup>, while frames b-d have been multiplied by 10<sup>5</sup> on the y-axis. See text for details.

[Title Page](#)[Abstract](#)[Introduction](#)[Conclusions](#)[References](#)[Tables](#)[Figures](#)[◀](#)[▶](#)[◀](#)[▶](#)[Back](#)[Close](#)[Full Screen / Esc](#)[Print Version](#)[Interactive Discussion](#)

EGU

**Quantitative  $\text{CH}_2\text{I}_2$   
vapor spectrum**

T. J. Johnson et al.

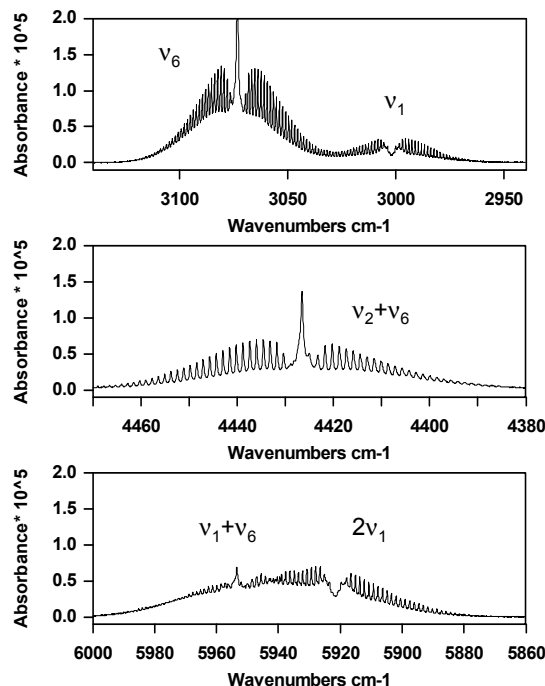


**Fig. 2.** Details of three  $\text{CH}_2\text{I}_2$  spectral regions of interest for monitoring. The spectra are all pressure broadened to 760 Torr and are composite spectra that correspond to 1 ppm-m optical depth. The y-axis is on the same scale in all three frames. Frame (a) shows the  $\nu_1$  band (3002  $\text{cm}^{-1}$ ) along with the  $\nu_6$  band (3073  $\text{cm}^{-1}$ ), frame (b) shows the  $(\nu_2 + \nu_6)$  combination band at 4427  $\text{cm}^{-1}$ , while frame (c) shows the  $2\nu_1$  overtone band (5921  $\text{cm}^{-1}$ ) along with the  $(\nu_1 + \nu_6)$  combination band at 5953  $\text{cm}^{-1}$ .

[Title Page](#)[Abstract](#)[Introduction](#)[Conclusions](#)[References](#)[Tables](#)[Figures](#)[◀](#)[▶](#)[◀](#)[▶](#)[Back](#)[Close](#)[Full Screen / Esc](#)[Print Version](#)[Interactive Discussion](#)

EGU

**Quantitative  $\text{CH}_2\text{I}_2$   
vapor spectrum**

T. J. Johnson et al.

[Title Page](#)[Abstract](#)[Introduction](#)[Conclusions](#)[References](#)[Tables](#)[Figures](#)[◀](#)[▶](#)[◀](#)[▶](#)[Back](#)[Close](#)[Full Screen / Esc](#)[Print Version](#)[Interactive Discussion](#)

EGU

Blue: 10 Torr  $\text{H}_2\text{O}$ ,  
Green: 1.8 ppm  $\text{CH}_4$ , Pink: 1 ppm  $\text{CH}_2\text{I}_2$

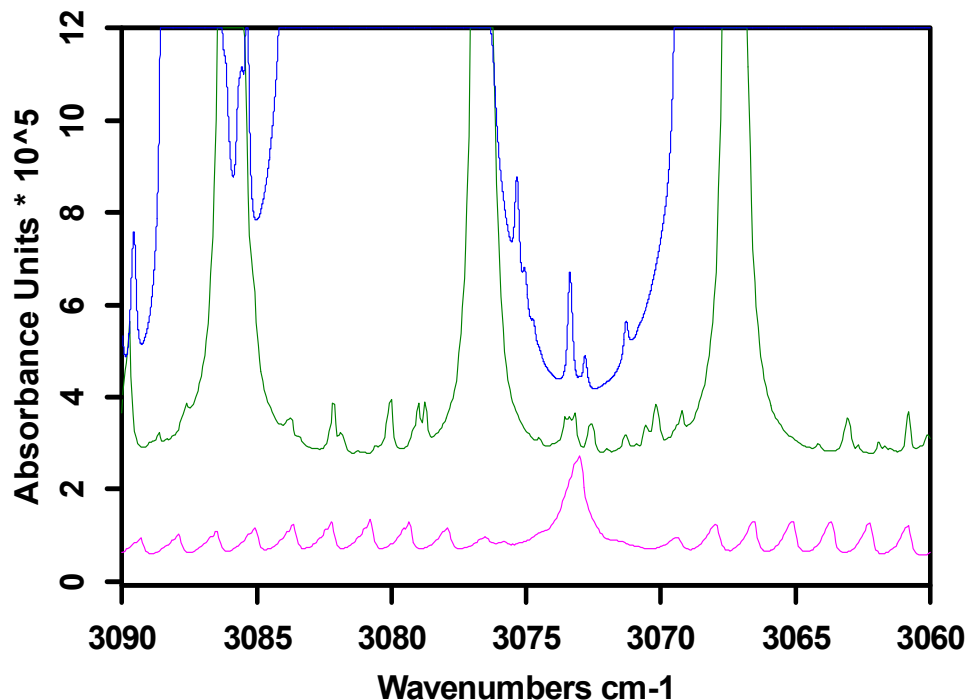


**Fig. 3.** Comparison plot (all at  $0.1\text{ cm}^{-1}$  resolution) showing potential interferents to the  $\text{CH}_2\text{I}_2$   $\nu_6$  band at  $3073.01\text{ cm}^{-1}$ . The traces correspond to 1 ppm-m of  $\text{CH}_2\text{I}_2$  (lower trace – pink), 1.8 ppm-m of  $\text{CH}_4$  (middle trace – green), and 10 Torr of  $\text{H}_2\text{O}$  (upper trace – blue). The  $\text{H}_2\text{O}$  data are from the HITRAN data base. The spectra have been vertically offset for clarity. See text for details.

**Quantitative  $\text{CH}_2\text{I}_2$   
vapor spectrum**

T. J. Johnson et al.

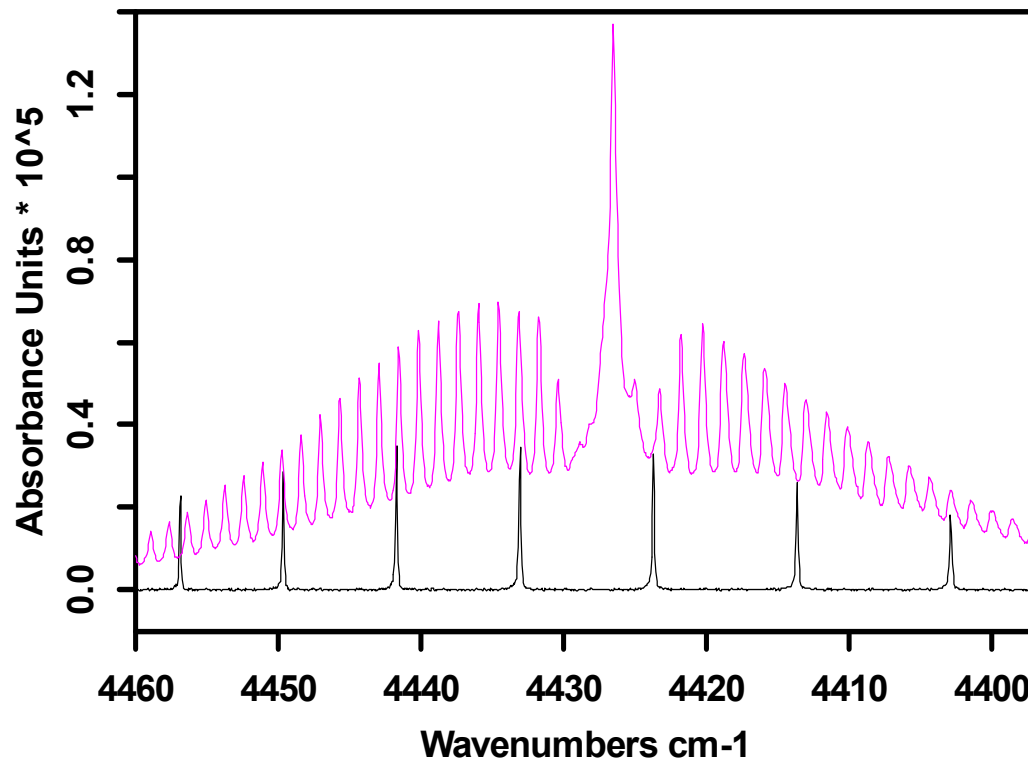


**Fig. 4.** Comparison plot (all at  $0.1\text{ cm}^{-1}$  resolution) showing potential laser combination measurements using the  $\text{CH}_2\text{I}_2$  ( $\nu_2 + \nu_6$ ) combination band at  $4426.52\text{ cm}^{-1}$ . The traces correspond to 1 ppm-m of  $\text{CH}_2\text{I}_2$  (upper trace – pink), and 1 ppm-m of hydrogen iodide, HI (lower trace – black). The spectra have been vertically offset for clarity. See text for details.

[Title Page](#)[Abstract](#)[Introduction](#)[Conclusions](#)[References](#)[Tables](#)[Figures](#)[◀](#)[▶](#)[◀](#)[▶](#)[Back](#)[Close](#)[Full Screen / Esc](#)[Print Version](#)[Interactive Discussion](#)

EGU



**Quantitative  $\text{CH}_2\text{I}_2$   
vapor spectrum**

T. J. Johnson et al.

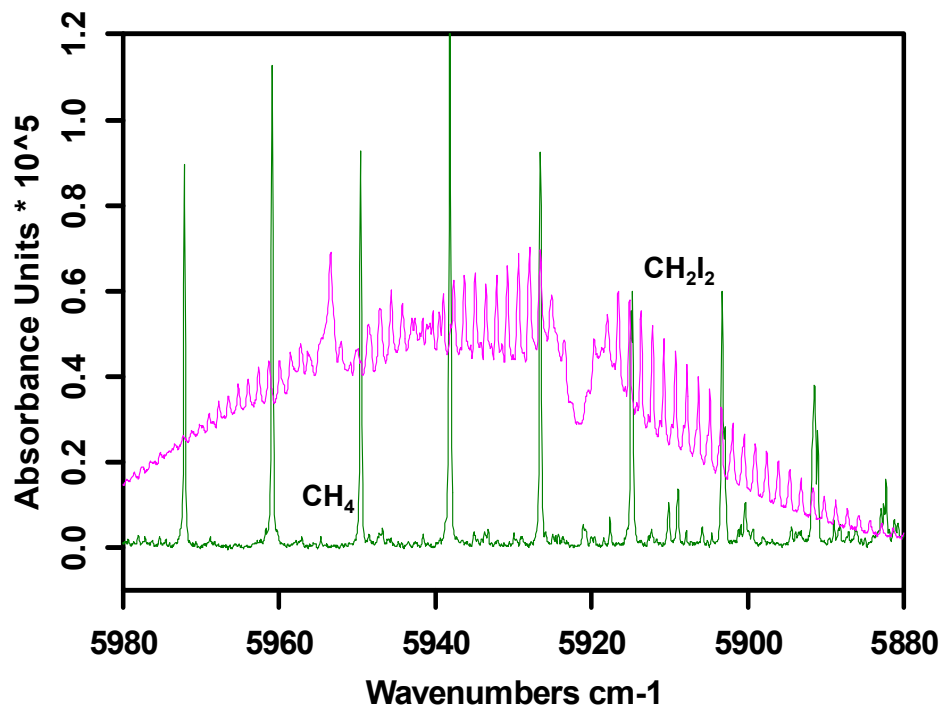


**Fig. 5.** Comparison plot ( $0.1\text{ cm}^{-1}$  resolution) showing potential laser combination measurements using the  $\text{CH}_2\text{I}_2$   $2\nu_1$  overtone band ( $5921\text{ cm}^{-1}$ ) along with the  $\nu_1 + \nu_6$  combination band at  $5953\text{ cm}^{-1}$  along with the potential interference from  $\text{CH}_4$ . The traces correspond to 1 ppm-m of  $\text{CH}_2\text{I}_2$  (upper trace – pink), and 1.8 ppm-m of methane,  $\text{CH}_4$  (lower trace – green). The spectra have been vertically offset for clarity. See text for details.

[Title Page](#)[Abstract](#)[Introduction](#)[Conclusions](#)[References](#)[Tables](#)[Figures](#)[◀](#)[▶](#)[◀](#)[▶](#)[Back](#)[Close](#)[Full Screen / Esc](#)[Print Version](#)[Interactive Discussion](#)

EGU